

Transcriptional mapping and genomic analysis of the cardiac atria and ventricles

XIAO-SONG ZHAO, TERESA D. GALLARDO, LING LIN,
JEFFREY J. SCHAGEMAN, AND RALPH V. SHOHEIT
*Department of Internal Medicine, University of Texas
Southwestern Medical Center, Dallas, Texas 75390-8573*

Submitted 19 July 2002; accepted in final form 28 October 2002

Zhao, Xiao-Song, Teresa D. Gallardo, Ling Lin, Jeffrey J. Schageman, and Ralph V. Shoheit. Transcriptional mapping and genomic analysis of the cardiac atria and ventricles. *Physiol Genomics* 12: 53–60, 2002; 10.1152/physiolgenomics.00086.2002.—The atria and ventricles of the heart have distinct development, structure, and physiology. However, only a few of the genes that underlie the differences between these tissues are known. We used a murine cardiac cDNA microarray to identify genes differentially expressed in the atria and ventricles. The reliability of these findings is supported by highly concordant repetition of hybridization, recognition of previously known atrial and ventricular isoforms of contractile proteins, and confirmation of results by quantitative PCR and in situ hybridization. We examined the most differentially regulated genes for evolutionarily conserved noncoding sequences and found that atrial-expressed genes have more predicted myocyte enhancer factor-2 (MEF2) binding sites than ventricle-predominant genes. We confirmed that messages for MEF2 family members are more abundant in the atria, as are their protein products. Moreover, the activity of a transgenic reporter construct for MEF2 activity is preferentially upregulated in the atria in response to hypertrophic stimuli. This study provides a greater understanding of the molecular differences between atria and ventricles and establishes the framework for an anatomically detailed evaluation of cardiac transcriptional regulation.

atrium; gene expression; microarray; myocyte enhancer factor 2

DEVELOPMENT OF THE VERTEBRATE heart begins when a sheet of mesoderm specified for cardiac development forms a crescent that folds toward the ventral midline to create a linear tube. At the eighth day of embryogenesis in the mouse, the distinction between ventricular and atrial myocardium is first recognized. At this time the linear heart begins to function as a pump. The atria remain thin-walled, receiving venous return at low pressure; while the ventricles begin to thicken by both hyperplasia and hypertrophy, pumping blood against a higher afterload (3).

Article published online before print. See web site for date of publication (<http://physiolgenomics.physiology.org>).

Address for reprint requests and other correspondence: R. V. Shoheit, Dept. of Internal Medicine, UT Southwestern Medical Center, Dallas, TX 75390-8573 (E-mail: ralph.shoheit@utsouthwestern.edu).

Anatomists have previously defined structural and ultrastructural differences between the upper and lower chambers of the heart. The Golgi apparatus and associated atrial granules are more prominent components in atrial myocytes. The sarcoplasmic reticulum in atrial cells is more complex and robust, whereas the transverse-axial tubular system is poorly developed compared with its ventricular counterpart (10). A distinct endocrine role has been long recognized for the atria. The thin, easily distensible wall, thick endocardium, and abundant granules containing ANP allow the atria to both monitor and modify intravascular volume. Finally, and most obviously, the pressure in the atria normally only rises to about 10 mmHg while ranging from 10 to 120, or higher, in the ventricle. This produces (and requires) a large difference in the proportion of cellular proteins and energy utilization devoted to contraction.

Some of the regional variation in gene expression that underlies these functional differences is known. There are a handful of relatively highly expressed and well-characterized genes for which transcriptional differences have been recognized and even functional effects described (reviewed in Refs. 11 and 16). For example, substitution of ventricular for atrial myosin light chain isoforms is sufficient to confer ventricular-like calcium sensitivity and cross-bridge cycling characteristics on atrial cardiomyocytes (27). Differences in depolarization and contractility between the atria and ventricles have been ascribed to differential regulation of several genes including angiotensin II receptor subtypes (31), sarcoplasmic reticulum calcium ATPase (24), potassium channel related genes (4, 7, 32), and phospholamban (2, 19).

To more comprehensively evaluate the molecular basis for the differences between the atria and ventricles, we used a deeply representative, cardiac-specific, cDNA microarray to compare the transcription profiles between atria and ventricles and identify those transcripts that are differentially expressed between the two tissues. We then examined these differentially regulated genes for transcription factor binding motifs within evolutionarily conserved noncoding regions that could confer chamber-specific regulation of expression. Finally, we demonstrated the greater atrial abundance and transcriptional activity of one of these transcription factors identified as a candidate for contributing to

differential gene expression between the atria and ventricles.

MATERIALS AND METHODS

Microarray creation. Libraries were created from cardiac and skeletal muscle RNA obtained from young adult mouse tissues (male and female). mRNA was prepared with TRIzol reagent (Invitrogen, Carlsbad, CA) and oligo-dT resin (Qiagen, Valencia, CA) according to the manufacturer's protocols. Two micrograms of mRNA was converted to cDNA and subcloned into pAMP10 (Invitrogen, Carlsbad, CA). Eight-thousand clones of each library were picked and grown on high-density filters. Insert was prepared from 30 of these clones, batch labeled by random priming with [³²P]dCTP, and used to probe the library. Hybridizing clones were removed from subsequent consideration, and the process was repeated until each clone in the probe was only recognizing an average of 1.2 of the remaining clones (10 iterations). Remaining clones were sequenced by dideoxy chain termination ("Big Dye" chemistry and 377 apparatus; PerkinElmer, Boston, MA) and mapped back to Unigene consensus sequences. A total of 1,706 independent clones were identified in the cardiac library and 3,982 in the skeletal muscle. Also, two previously characterized IMAGE consortium libraries (20) were purchased (Soares, Image ID 397; Stratagene, Image ID 290; Incyte Genomics, Palo Alto, CA). The available sequence information was confirmed in a sample of 96 clones from each library. Accession numbers were used to obtain Unigene identifications with Arrogant gene collection management software (available at <http://lethargy.swmed.edu>). The "refseq" identification was used to parse unique sequences from the library clones. Our criteria for nonredundancy were fulfilled by 3,704 clones from the fetal cardiac library and 2,306 clones from the adult cardiac library. We did not remove interlibrary redundancy, both to maintain duplicate clones on the array and to prevent removal of library-specific isoforms. In total, 7,716 heart clones were applied to the array. In silico comparisons show that ~5,000 independent cardiac genes are represented in this collection. Details of library construction and all target clones can be found at <http://pga.swmed.edu>. Plasmid DNA was isolated from these clones and inserts were amplified with M13 primers. After ethanol precipitation, these inserts were resuspended in 7% DMSO and spotted onto poly-lysine-coated microscope slides. These slides were postprocessed with UV cross-linking and succinic anhydride blocking as previously described (6).

RNA extraction, hybridization, and quantification. Hearts were harvested from 6- to 8-wk-old male C57BL/6 mice, and the atria and ventricles were carefully separated under a dissecting microscope. Total RNA was isolated with TRIzol reagent according to the manufacturer's protocol. Probes were prepared from 20 µg of pooled total RNA by reverse transcription primed with oligo-dT (Superscript II, GIBCO-BRL) incorporating Cy3 or Cy5. The labeled probes were combined, concentrated on a 30 kDa size-exclusion filter (Amicon) and brought to a final volume of 50 µl of 3× SSC/0.3% SDS containing 10 µg of poly-A RNA and 10 µg of mouse *CotI* DNA. Hybridization was carried out in a slide chamber in 62°C water bath overnight. Slides were washed to a final stringency of 0.1× SSC at room temperature. They were read in a GenePix scanner at photomultiplier tube settings that produced equivalent signal in both channels and low background. Data were imported into an automated spreadsheet where a background threshold, based on several hundred blank solvent spots scattered through the array, was determined for each hybridization and mean log ratio

normalization was performed (8) [the Marc-V program (28) is available for download at <http://pga.swmed.edu>]. Highly regulated genes were resequenced to confirm identity and obtain more complete sequence information on expressed sequence tags (ESTs).

Array results were confirmed by real-time PCR assays. We designed oligonucleotide primers from the cDNA sequence that were predicted to cross an intron (see Table 2); if the mouse gene organization was not available, then we used homology to the human gene. All amplicons were initially resolved on a 2% agarose gel to confirm that only a single product was generated. These primers were used to amplify product from cDNA representing 5 ng of total RNA. PCR was run in triplicate with SYBR green fluorophore (Molecular Probes, Portland, OR) in a Opticon device (MJ Research, Waltham, MA). Expression level was interpolated from a standard curve generated from a series of dilutions at cycle times where threshold intensity was clearly exceeded. Glycerinaldehyde-3-phosphate dehydrogenase was used as an internal control. A standard two-phase reaction (95°C for 15 s, 60°C for 1 min) worked for all amplifications.

Animal manipulations. Generation of the myocyte enhancer factor-2 (MEF2) activity indicator mouse was reported previously (25). Male, 6- to 8-wk-old transgenic mice were treated with isoproterenol (15 mg·kg⁻¹·day⁻¹ for 7 days) (30), angiotensin II (200 ng·kg⁻¹·min⁻¹ for 7 days) (15), or saline by osmotic minipump (Alzet, model 1007D), implanted during Avertin anesthesia. Hyperthyroidism was obtained by daily intraperitoneal injection (triiodothyronine, 1 µg·g⁻¹·day⁻¹ for 7 days) (17).

Histology. Mouse hearts were embedded in tissue freezing medium (Triangle Biomedical Sciences, Durham, NC), and 5-µm sections were obtained in a four-chamber plane with a cryostat. These sections were incubated first with antibody to the carboxy terminus of MEF2 (sc-313, Santa Cruz Biotechnology), and binding was revealed with FITC-labeled secondary antibody (Fisher Scientific, Pittsburgh, PA). Counterstaining with propidium iodide indicated the location of nuclei. Subcellular localization of MEF2 signal was obtained with "nearest-neighbor" deconvolution software (OpenLab version 2, Improvision) on a Zeiss Axiovert 100M model inverted microscope. For detection of β-galactosidase, hearts were briefly fixed in 2% paraformaldehyde/0.2% glutaraldehyde in PBS on ice for 90 min followed by incubation in X-gal staining solution [5 mM potassium ferrocyanide, 5 mM potassium ferricyanide, 2 mM MgCl₂, 1 mg/ml 5-bromo-4-chloro-3-indolyl-β-D-galactopyranoside (X-gal) in dimethylformamide] at room temperature overnight. In addition, from a subset of animals in each group, 200-µm sections were obtained with a Vibratome (Energy Beam Sciences, Agawam, MA) and stained with X-gal substrate in a similar manner.

In situ hybridization was performed to identify the location of gene expression as previously described (29). Briefly, riboprobes were generated, from the plasmids used to create the array targets, using T7 or Sp6 RNA polymerase (Maxi-script; Ambion, Austin, TX) according to the manufacturer's recommendations. They were applied over deparaffinized heart sections that had been briefly microwaved and Pronase E-treated to help unmask RNA. Hybridization was conducted for 14 h at 55°C in 50% formamide, 0.3% dextran, 1× Denhardt's solution, 0.5 mg/ml tRNA, and 7.5 × 10⁵ cpm of the probe. The slides were then washed to a final stringency of 65°C in 50% formamide/2× SSC for 30 min. K.5 nuclear emulsion (Ilford Imaging, Paramus, NJ) was applied to the slides, which were then exposed at 4°C for 14 days.

Immunoblotting. Atria and ventricles were homogenized in RIPA buffer (50 mM Tris, 150 mM NaCl, 1 mM EDTA, 1

Table 1. Genes differentially expressed in atria vs. ventricles

Accession No.	Gene Name	Fold Regulation
<i>Atrium > Ventricle</i>		
AA073254	Myosin light chain, 1A (4)	31(25–40)
AA419767	Myosin light chain, 2A (5)	22(14–36)
AA139662	Atrial natriuretic factor (4)	15(12–18)
Mm.27151*	EST	14(8.8–21)
AA755962	EST novel†	12(4.8–31)
AA789894	EST	11(8.4–13)
BG794401	Glutathione peroxidase (4)	10(7.4–14)
Mm.603*	SnrpD1	6.4(4.3–9.6)
BG792204	Clusterin/apolipoprotein J (5)	6.1(3.6–10)
BG791545	Sarcophilin (3)	5.9(2.3–16)
AA139889	Retinoblastoma binding protein-4	4.8(0.6–40)
AA073572	Connective tissue growth factor	3.9(2.9–4.9)
Mm.39706*	EST	3.6(2.3–5.6)
AA795393	Transient receptor protein 2 (2)	3.5(2.6–4.6)
AA756195	EST	3.4(2.8–4.2)
BG794713	Elongation factor 1-alpha (8)	3.3(2.0–5.0)
BG796916	EST	3.3(2.7–4.1)
AI639666	EST	3.2(1.5–7.1)
AA073904	Dickkopf homolog 3 (2)	3.1(1–10)
BG796603	Gelsolin (12)	3.0(2.8–3.2)
<i>Ventricle > Atrium</i>		
AA530365	EST	34(21–55)
BG791717	Myosin light chain-2V (7)	23(13–42)
BG795128	K+ channel modulatory factor (Debt91)	11(2.8–40)
BG791806	Myosin light chain-1V (5)	10(6.0–17)
AA499092	EST	9.7(6.4–15)
AA139890	Ribosomal protein S17 (2)	5.4(3.2–9.1)
AA759870	Protein tyrosine kinase 3	4.8(1.8–13)
AA499179	EST	4.7(2.5–8.8)
BG791857	Four and a half LIM domains 2 (3)	3.8(2.6–6.8)

Data presented are specific to the clone with the accession number provided. The number of clones on the array that showed similar regulation is provided in parentheses after the gene name. Fold regulation is shown with 95% confidence intervals in parentheses. *Unigene cluster has been substituted when accession number was indeterminate after resequencing. †EST denoted as novel has no homology to any other gene or EST in the public databases.

mM EGTA, pH 7.4) supplemented with 1% Nonidet P-40, PMSF (0.2 μM), leupeptin (10 μg/ml), and pepstatin (10 μg/ml). The lysate was cleared by centrifugation, and 10 μg of protein (determined with Bradford reagent; Bio-Rad Laboratories, Hercules, CA) was subjected to electrophoresis in a 10% SDS polyacrylamide gel and transferred onto PVDF membranes. The blots were incubated with a 1:2,000 dilution of the same anti-MEF2 antibody used for immunohistochemistry, followed by HRP-labeled secondary antibody (Fisher Scientific, Pittsburgh, PA). The signals were detected by SuperSignal chemiluminescent reagent (Pierce Endogen, Rockford, IL).

Bioinformatic analyses. Mouse and human gene sequences were extracted from either National Center for Biotechnology Information (NCBI) or Celera databases. We were able to obtain adequate sequence data from both species to analyze 17 of the atrial-expressed genes and 6 of the ventricular-expressed genes. We added a further 29 genes with a ventricle-to-atrial expression ratio of between 1 and 3 amenable to this analysis. We used rVISTA software (22) to identify predicted transcription factor binding sites within 5 kb up-

stream and downstream of the gene. The default parameters used with this program included a TRANSFAC search with core similarity 0.75, matrix similarity 0.8, and evolutionary conservation (80% similarity) of the neighboring 24-bp window of sequence. We have included a predicted MEF2 site in a non-atrial-specific gene (myomesin 1) even though it was not within a long evolutionarily conserved noncoding sequences (NCS), simply because the rVISTA software, using a moving window of similarity, detected a match. If we had not included this gene in our analysis, then the statistical significance of our findings would be even more impressive.

Statistics. Expression data for each of the results shown (Table 1) were generated from the average of four independent determinations obtained from the hybridization target on the array. We calculated confidence intervals from the standard deviation of these averaged expression ratios using a standard *t*-test (shown as a range for fold change). Pearson correlation was used to compare the overall similarity of the hybridization result from entire arrays. A Fisher exact test was used to check the significance of differences in abundance of predicted transcription factor binding sites between groups of genes.

RESULTS

We used a tissue-specific cDNA microarray to compare RNA samples from pooled atria and ventricles. Two sets of dye-reversal cDNA microarrays (four arrays) comparing atria and ventricles were used to calibrate each gene. The results of the hybridizations were highly similar. Pearson correlation for all results on the array was 0.78 when atrial RNA was labeled with Cy3 and 0.82 when atrial RNA was labeled with Cy5. Fluorescence intensities of 670 target spots had >1.8 fold differential expression in either direction in any hybridization. The four results were averaged for each of these clones. After confirmation and resolution of redundancy, 9 genes were more than 3-fold more abundant in ventricle, and 20 genes were more than 3-fold more abundant in atrium. Of these 29 substantially differentially regulated genes, 19 were known genes and 10 were similar only to otherwise uncharac-

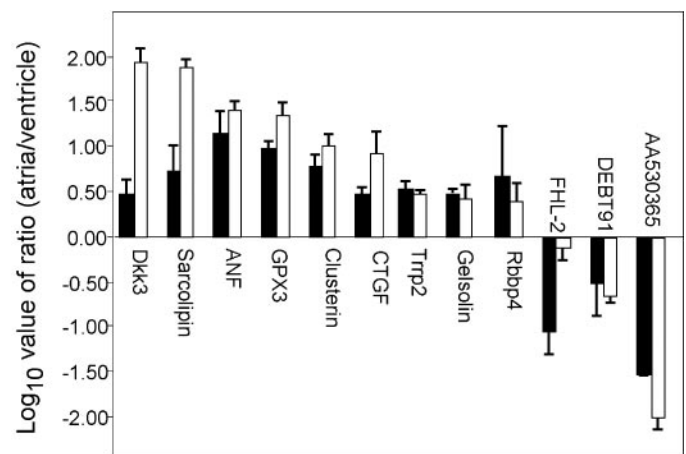


Fig. 1. Comparison of microarray and real-time PCR results. The two results are shown for the 12 highly regulated genes for which real-time data was obtained (microarray in black, real-time in white). The direction of regulation was confirmed in all genes tested, although the degree of regulation can vary as shown.

terized ESTs. One of the anonymous ESTs was entirely novel, with no homolog in any database. Results and 95% confidence intervals were determined for the fold change of each of these genes and are shown in Table 1. Among the most differentially expressed genes were the expected atrial-specific transcripts for atrial natriuretic factor (ANF) and the atrial and ventricular isoforms of myosin light chain. We confirmed differential expression of 12 of these genes by real-time PCR. The

results show excellent correlation of array and PCR results (Fig. 1).

The expression pattern of several genes of particular interest was defined by in situ hybridization (Fig. 2). The atrial isoform of myosin light chain gave the expected intense atrial-specific signal localized over myocytes. Other probes showed atrial-specific expression concentrated in myocytes, vascular endothelium, parietal pericardium, or other cellular components. Not all

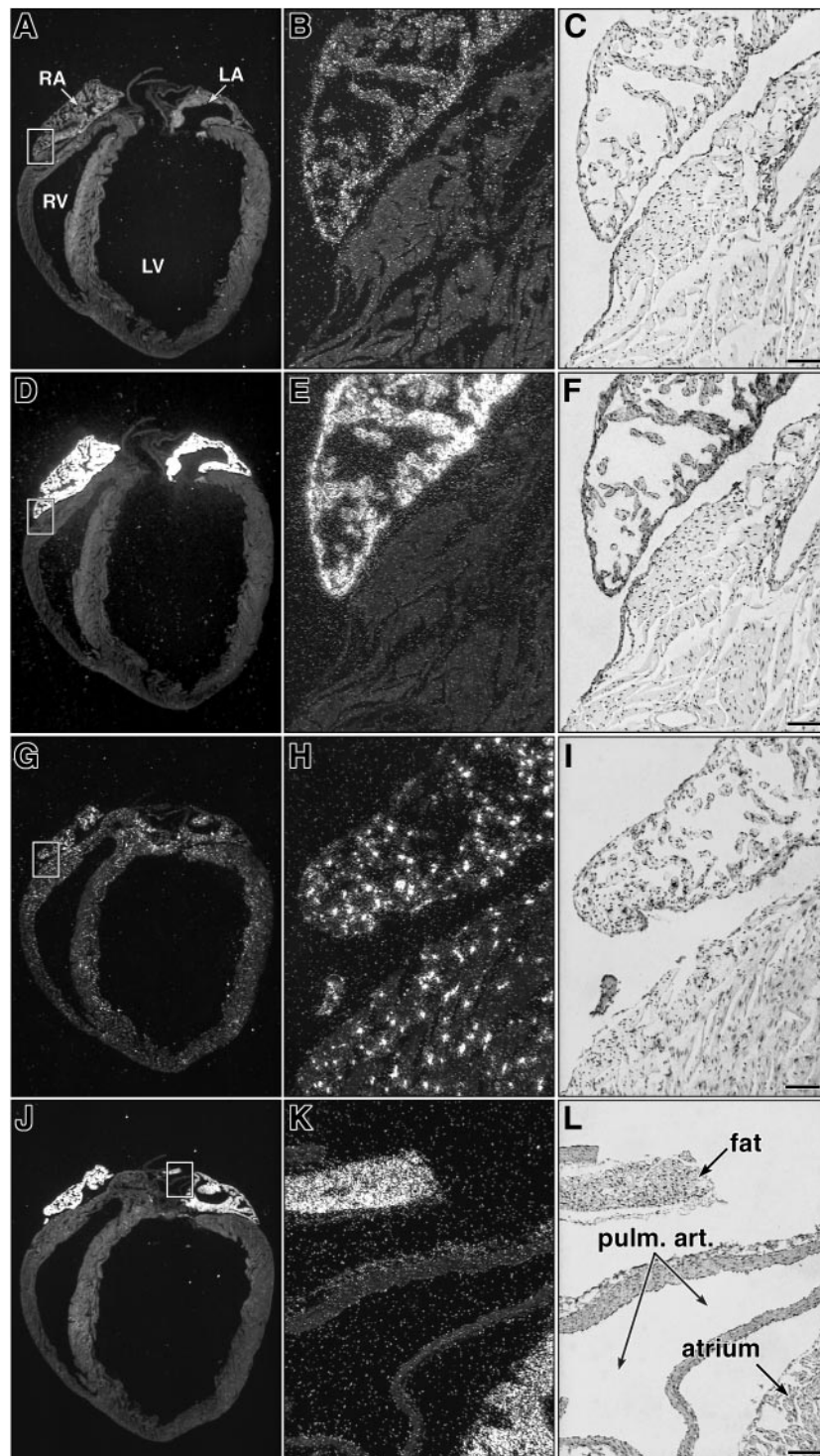


Fig. 2. In situ hybridization of atrial-specific transcripts. The left column shows 4 chamber sections of adult mouse heart with in situ hybridization of EST vv36h12 (A–C), myosin light chain 1A (D–F), gelso-lin (G–I), or glutathione peroxidase 3 (J–L). The middle column shows higher magnification views that localize signal to the atrial myocytes (B and E), the fibroblasts (H), or the myocytes and pericardiac fat (K). The right column shows bright-field images of the same sections that allows this more precise histological evaluation (bar in L = 100 μ m). RA and LA, right and left atrium, respectively; RV and LV, right and left ventricle, respectively.

Table 2. *Oligonucleotides used for real-time PCR*

Name	Forward Primer	Reverse Primer
ANF	AGAAACCAGAGAGTGGCAGAG	CAAGACGAGGAAGAAGCCCAG
AA530365	GTTTGTACCCAAACATAGGGCC	CACAACATGTGGTAGAGGCACC
AA789894	TCCCGTACTCCTCATCATCACC	AATTTGTTGAATCTGCAGGACTAGG
Abcd4	CCTTGAGAAGTTCCTCCTGGG	TCCGCTGCTCAGATGAACC
Atp5c1	CTGCAAAGTATGCCCGGG	CCTCAGGTGCCTTAATATCAGCC
Bak1	TCATCGGAGATGATTAACCGG	GCTGATGCCACTTTAAATAGGC
BNP	CCAGTCTCCAGAGCAATTCAAGAT	GCTAATTCACAAAGGACTCGAGGT
Clusterin	GTCTCCACCGTGACCACCC	CTGGTAACACCACTGTGATGGG
CTGF	CCGAGAAGGGTCAAGCTGC	TGTGTCTTCCAGTCGGTAGGC
Debt91	CAGCGTTATCCAATGGTTACTGGC	CCTGGGTTCCACTGCAGAGC
Dkk3	AGAGGAGCCATGAATGTATCATTG	TCGGGTGCATAGCATCTGC
FHL2	AAGGAGAATCAGAACTTCTGCGTG	CGGTAAGTAACACCTCCTGTGGT
GAPDH	TGCACCACCAACTGCTTAG	GGATGCAGGGAT GATGTTT
Gelsolin	CAGACAGCTCCTGCCAGTATCC	GAGTTTCAGAGCACCAGACTTAGGC
GPX3	TACTCCCCAGTCTCAAGTATGTTTCGACC	TTCTGCAGTGGGAGGGCAGG
MEF2A	AAGTACCGGCAGTGCAAGTGG	CCCTTGAGTTTACAATCCATTCC
MEF2B	AACGCCTCTTCCAGTATGCC	CTCCTCTTAAGTGTCTGAAGGATATCC
MEF2C	GATGCCATCAGTGAATCAAAGG	GTTGAAATGGCTGATGGATATCC
MEF2D	CCCCTGCCTACAACACAGATTACC	GCGGTGACATTGCCCTAGTGC
Mm.27151	GTTGGTTGATGTCTTGTGCGAAGG	GAGTATCAGTGCAGCTTACAACACAGC
Mm.39706	GGCTCCTAACTTATGCTGAGATCG	AGCCTGGTCATCCCAAACC
MLC 1A	GCATGTCCTTGCTACCCTGG	AAAGGCTTCATAGTTGATGCAGC
MLC 2A	TCAAGGAAGCCTTCCAGTGC	CGGAACACTTACCCTCCCG
Myomesin 1	AGTTAACTGGTCCCACAATGGG	GAGTGGGCTCGTTGATCTGC
Rbbp4	CTATAAGCCCAAACCACCGG	AAACCAGACTTTGTTCAGCTACCC
Sarcolipin	GGGCCATGCTATACTCCAGGG	GTGGGTGAGAGATGCTGGAGG
Trpp2	ATACCATTGCTCGGCCCCAC	GGTGTGATTCCGGGATAGTGAGAAC

gave signal greater than background; those that did confirmed the direction of expression in 9 of 10 genes.

To search for *cis*-acting regulatory sequences in atrial and ventricular highly regulated genes, we used rVISTA (“regulatory visualization tool for alignment,” <http://pga.lbl.gov/rvista.html>) to compare the mouse and human sequences of the genes. This software looks at evolutionarily conserved transcription binding factor sites, includes a flexible criterion for alignment within noncoding sequences, and appears to reduce false-positive predictions of binding sites. The result of this analysis showed 4 of the 17 atrial-expressed genes to have conserved MEF2 sites, whereas only one of 35 ventricular-predominant genes had a conserved site ($P_{\text{exact}} = 0.05$, Table 3).

Table 3. *Predicted MEF2 sites in evolutionarily conserved noncoding sequence*

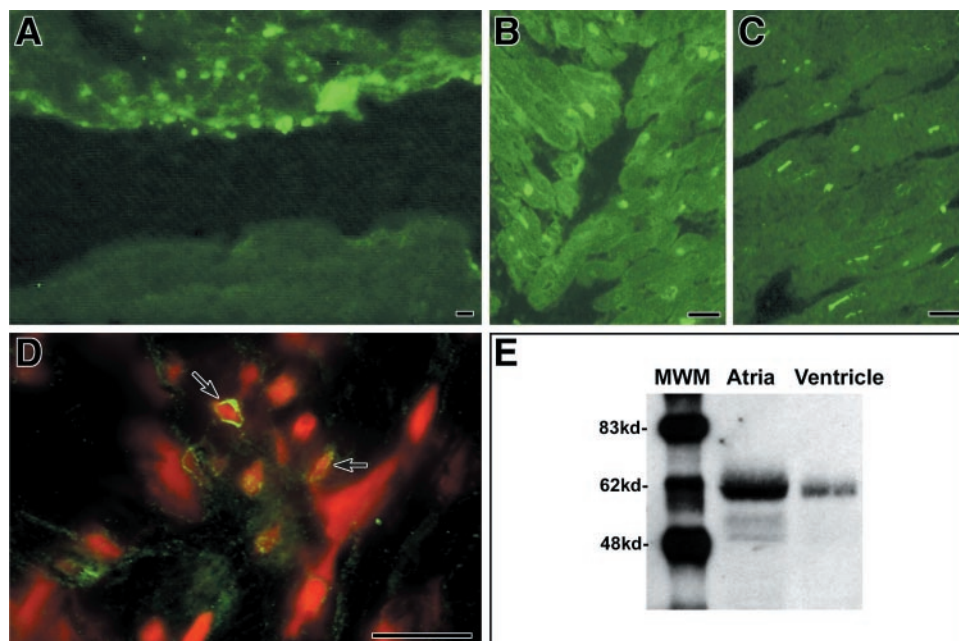
Chamber Specificity	Number of Genes	Genes with MEF2 in Noncoding Sequences		BP of Sequence Analyzed
		+	-	
Atrium > 3-fold	17	4*	13	157,180
Ventricle > 3-fold	6	0	6	169,809
Ventricle 1- to 3-fold	29	1†	28	471,182

* Atrial-specific genes with conserved MEF2 sites by rVISTA analysis are mm27151, retinoblastoma binding protein 4, AA789894, and sarcolipin. † Myomesin 1 has a 1:1 atrial-ventricular expression ratio. The difference in frequency of MEF2 sites between atrial-expressed and ventricle-expressed genes is significant at $P_{\text{exact}} = 0.05$ by the Fisher exact test.

The array contained cDNAs for the four isoforms of MEF2 (1). Hybridization signal was low for these cardiac transcription factors, close to the overall threshold used for the general analysis of the array data. Nonetheless, those targets that gave signal greater than background suggested that MEF2 isoforms might be more abundant in atria than ventricles, with ratios of atrial to ventricular expression of 1.4, 1.2, 1.2, and 1.3 for MEF2A, -2B, -2C, and -2D, respectively. We then examined expression levels of MEF2 by real-time PCR with oligonucleotides that distinguished the various isoforms. This established that MEF2A, -2B, -2C, and -2D were 2.1, 1.5, 2.7, and 2.0-fold higher in atria than ventricles, respectively. By Western blotting we found that MEF2 proteins are more abundant in atria than in ventricles (Fig. 3E). The antibody used recognizes MEF2A, -2C, and -2D, and the principal band seen on the Western blot has an implied molecular weight most consistent with MEF2A (18). Immunohistochemistry confirmed that MEF2 protein is located in myocytes with more intense signal in atria than in ventricles. Higher resolution images obtained with deconvolution software show that the MEF2 is found predominantly in discreet sublaminal regions of the nucleus (Fig. 3D).

To assess the functional role of elevated levels of MEF2 in the atria we used a “MEF2 indicator animal” that has a transgene with concatamerized MEF2 binding sites (taken from the desmin gene) upstream of a β -galactosidase reporter construct (25). At baseline there was little β -galactosidase activity in either the atrium or ventricle. After stimulation with the hypertrophic agents isoproterenol, angiotensin II, and thyroid hormone, β -galactosidase activity was detected

Fig. 3. Protein level of myocyte enhancer factor-2 (MEF2) in atria and ventricles. *A*: low-power magnification of atrium (*top*) and ventricle (*bottom*) with immunostaining of MEF2 much more abundant in atrial cardiocytes. Higher magnification views of atrium (*B*) and ventricle (*C*) show more atrial MEF2 staining in both nuclei and cytoplasm. *D*: the colocalization of MEF2 staining (yellow, FITC) and nuclei (red, propidium iodide). MEF2 is mainly localized to the circumference of the nuclear membrane. Western blot analysis (*E*) shows MEF2A (and possibly MEF2D), migrating near 60 kDa, and MEF2C, at about 50 kDa, substantially more abundant in the atria than ventricles (size bars = 15 μ m).



and was substantially greater in the atria than in the ventricles (Fig. 4). We did not detect any increase in MEF2 protein by Western blotting with these stimuli (data not shown), suggesting that the increase in activity may be due to posttranslational activation of MEF2, as has been previously demonstrated (12, 23). We confirmed that the greater staining seen in the atria was not a technical artifact of access to substrate by repeating the β -galactosidase assay on fresh Vibratome sections of heart (data not shown).

We then explored whether the increased MEF2 activity observed with isoproterenol stimulation was reflected in regulation of putative target genes in the

atrium. We examined four categories of genes: atrial-predominant genes with 1) at least one MEF2 site in an evolutionarily conserved sequence, 2) at least one MEF2 site with evolutionary alignment (but outside of a highly conserved region), 3) no MEF2 site recognized by the rVISTA software, and 4) genes without chamber specificity or ventricular predominance (and no aligned or conserved MEF2 sites). As shown in Table 4, seven of the 14 atrial-predominant genes showed >1.8-fold upregulation in the atria of isoproterenol-treated mice, and only one of the 7 genes examined with neutral or ventricular predominance was upregulated. However, among atrial-predominant genes, three of the six genes

Fig. 4. Cardiac MEF2 activity revealed by des-MEF2-LacZ transgenic mice. MEF2 indicator mice were challenged with saline (*A*), isoproterenol (*B*), angiotensin II (*C*), and thyroid hormone (*D*), and β -galactosidase activity was revealed by a histological stain. Atrial staining is more prominent than ventricular staining in all models (bar = 1 mm).

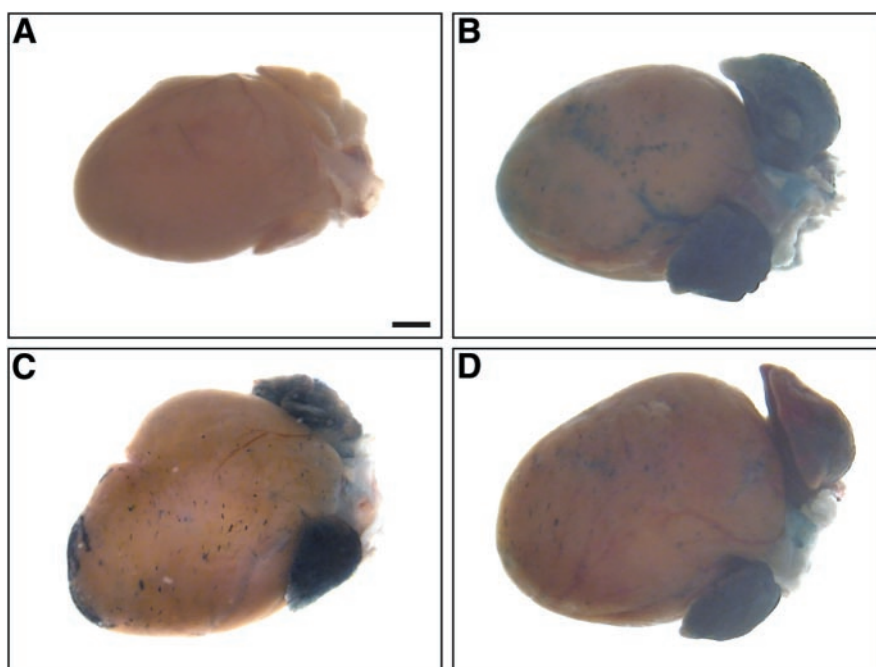


Table 4. Regulation of gene expression in the atrium in response to isoproterenol

Gene Name or Accession No.	Fold Change	Gene Name or Accession No.	Fold Change
1) MM.27151	1.6	12) GPX3	2.3
2) AA789894	2.2	13) Clusterin	1.8
3) RBBP4	1.0	14) Gelsolin	1.0
4) Sarcolipin	0.5	15) CTGF	5.9
5) Myomesin 1 (A:V=1:1)	2.6		
6) MLC1A	0.6	16) BAK1	1.0
7) ANF	1.0	17) ABCD5	0.7
8) DKK3	3.6	18) ETBR	0.7
9) MM.39506	1.8	19) ATP5C	0.7
10) MLC2A	0.4	20) BNP	0.5
11) TRP2	0.4	21) DEBT 91	0.5

mRNA abundance in pooled atria from mice treated with isoproterenol was determined by quantitative PCR. Fold regulation compared to untreated mice was normalized to GAPDH expression. Genes 1–4 have a MEF2 site in evolutionarily conserved noncoding sequence; genes 5–9 have an aligned MEF2 site outside of conserved regions; genes 10–15 have no identified conserved or aligned site; all genes 1–15 are more highly expressed in atrium than ventricle, except for myomesin as noted. Genes 16–21 have no MEF2 site in conserved noncoding sequence and are expressed equally in atrium and ventricle, or more abundantly in ventricle.

lacking evolutionarily conserved MEF2 sites showed such upregulation.

DISCUSSION

This study illustrates the power of a tissue-specific microarray to identify genes that are expressed in specific regions of the heart. The array data revealed 29 >3-fold differentially expressed genes including several of those previously shown to have differential expression in the atria and ventricles. Twenty of them are more abundant in atria, and nine are more highly expressed in ventricles. Many are novel or uncharacterized ESTs of unknown function. Some of the known genes may contribute to a physiological distinction between atria and ventricle. For example, the message for a homolog of sarcolipin is abundant in atria, whereas that of the related protein phospholamban is more abundant in ventricle. In fast skeletal muscle, sarcolipin regulates SERCA1, whereas phospholamban regulates SERCA2A in the heart (5). The abundance of the mRNA for the sarcolipin homolog in the atria, and the relative paucity of phospholamban, raises the intriguing possibility that this protein may play a role in regulating calcium pools in the atria, perhaps contributing to the distinct contractile attributes of atrial tissue (24). As the roles of genes that are regulated in a chamber-specific fashion is elucidated, they will provide further clues to the functional and structural differences between atria and ventricles.

Even for rare transcripts, such as MEF2 isoforms, the array produced data that was confirmed by other methods. Members of the MEF2 family of transcription factors bind a conserved AT-rich DNA sequence that is required for appropriate expression of many cardiac structural genes. When the MEF2C gene is completely

deleted, the heart tube does not undergo looping morphogenesis, and a subset of cardiac muscle genes are not expressed in embryonic heart, including ANF and MLC1A (which are found predominantly in the atrium in the adult animal) (21). Several of these MEF2-regulated genes are also upregulated in adult atria with hypertrophic stress. This suggests that the higher MEF2 levels identified in the atria contribute to dynamic, chamber-specific, transcriptional responses in the adult heart.

Distinct spatial segregation of gene expression occurs very early in cardiac development (reviewed in Ref. 3). During later embryonic development of the heart, there is likely to be an interplay of hemodynamic stimuli and developmental programming that determines chamber-specific gene expression. At parturition there is an abrupt change in afterload and filling pressures and continued structural remodeling of the cardiac chambers (9). Later in life, a variety of stresses can elicit transcriptional responses in the heart. These include structural remodeling that occurs with ventricular dysfunction and hypertrophy. In chronic atrial fibrillation there is a process of electrophysiological remodeling that makes the atrium resistant to defibrillation and reduces the likelihood of maintaining sinus rhythm (26). Here we have identified a large number of genes that are differentially regulated in a chamber-specific manner. Recent studies have shown that non-transcribed regulatory sequences tend to be evolutionarily conserved and support the use of comparative genomics as an effective tool for the discovery of biologically active gene regulatory elements (13, 14, 33). We have examined the sequence of these coordinately expressed genes to identify conserved transcription factor binding sites that might confer chamber specificity and confirmed that transcriptional activity of one of these factors is indeed higher in the atria. Interestingly, many atrial-specific genes are upregulated by the isoproterenol stimulus regardless of whether they have an identified MEF2 site in an evolutionarily conserved position. Our interpretation of these data (based on this relatively small sample of genes), is that atrial-predominant genes are more responsive to adrenergic stimulation as a class. This in turn suggests a “transcriptional field” defined by a chamber-specific mélange of transcription factors, which includes MEF2, that are enriched or more active in atrium. We think it likely that these transcription factors maintain both higher constitutive expression levels and the potential for greater responsiveness of atrial-predominant genes.

More work will be needed to establish the biological significance of evolutionarily conserved binding sites for transcription factors as well as the physiological significance of chamber-specific gene expression in the heart. The transcriptional mapping presented here provides the framework for greater refinement of therapeutic efforts utilizing gene regulation or expression. It also establishes the foundation for a more detailed understanding of normal and pathological regulation of cardiac gene expression.

We are grateful to Skip Garner for construction of the microarray spotter used in these studies and to John Shelton and James Richardson for expert histological advice and assistance. This work was supported by the National Heart, Lung, and Blood Institute (NHLBI) Program for Genomic Applications HL-66880, NIH/NHLBI RO-1-HL-64041, the Texas Higher Education Coordinating Board Advanced Technology Program, and an Innovation in Clinical Research Award from the Doris Duke Foundation.

REFERENCES

1. **Black BL, Martin JF, and Olson EN.** The mouse MRF4 promoter is trans-activated directly and indirectly by muscle-specific transcription factors. *J Biol Chem* 270: 2889–2892, 1995.
2. **Boknik P, Unkel C, Kirchhefer U, Kleideiter U, Klein-Wiele O, Knapp J, Linck B, Luss H, Muller FU, Schmitz W, Vahlensieck U, Zimmermann N, Jones LR, and Neumann J.** Regional expression of phospholamban in the human heart. *Cardiovasc Res* 43: 67–76, 1999.
3. **Chen JN and Fishman MC.** Genetics of heart development. *Trends Genet* 16: 383–388, 2000.
4. **Dixon JE and McKinnon D.** Quantitative analysis of potassium channel mRNA expression in atrial and ventricular muscle of rats. *Circ Res* 75: 252–260, 1994.
5. **East JM.** Sarco(endo)plasmic reticulum calcium pumps: recent advances in our understanding of structure/function and biology (review). *Mol Membr Biol* 17: 189–200, 2000.
6. **Eisen MB and Brown PO.** DNA arrays for analysis of gene expression. *Methods Enzymol* 303: 179–205, 1999.
7. **England SK, Uebele VN, Shear H, Kodali J, Bennett PB, and Tamkun MM.** Characterization of a voltage-gated K⁺ channel beta subunit expressed in human heart. *Proc Natl Acad Sci USA* 92: 6309–6313, 1995.
8. **Epstein CB, Hale W IV, and Butow RA.** Numerical methods for handling uncertainty in microarray data: an example analyzing perturbed mitochondrial function in yeast. *Methods Cell Biol* 65: 439–452, 2001.
9. **Fernandez E, Siddiquee Z, and Shohet RV.** Apoptosis and proliferation in the neonatal murine heart. *Dev Dyn* 221: 302–310, 2001.
10. **Forbes MS, Van Niel EE, and Purdy-Ramos SI.** The atrial myocardial cells of mouse heart: a structural and stereological study. *J Struct Biol* 103: 266–279, 1990.
11. **Franco D, Lamers WH, and Moorman AF.** Patterns of expression in the developing myocardium: towards a morphologically integrated transcriptional model. *Cardiovasc Res* 38: 25–53, 1998.
12. **Han J and Molkentin JD.** Regulation of MEF2 by p38 MAPK and its implication in cardiomyocyte biology. *Trends Cardiovasc Med* 10: 19–22, 2000.
13. **Hardison RC.** Conserved noncoding sequences are reliable guides to regulatory elements. *Trends Genet* 16: 369–372, 2000.
14. **Hardison RC, Oeltjen J, and Miller W.** Long human-mouse sequence alignments reveal novel regulatory elements: a reason to sequence the mouse genome. *Genome Res* 7: 959–966, 1997.
15. **Kato M, Egashira K, and Takeshita A.** Cardiac angiotensin II receptors are downregulated by chronic angiotensin II infusion in rats. *Jpn J Pharmacol* 84: 75–77, 2000.
16. **Kelly RG, Zammit PS, and Buckingham ME.** Cardiosensor mice and transcriptional subdomains of the vertebrate heart. *Trends Cardiovasc Med* 9: 3–10, 1999.
17. **Klein I.** Thyroxine-induced cardiac hypertrophy: time course of development and inhibition by propranolol. *Endocrinology* 123: 203–210, 1988.
18. **Kolodziejczyk SM, Wang L, Balazsi K, DeRepentigny Y, Kothary R, and Megeney LA.** MEF2 is upregulated during cardiac hypertrophy and is required for normal post-natal growth of the myocardium. *Curr Biol* 9: 1203–1206, 1999.
19. **Koss KL, Ponniah S, Jones WK, Grupp IL, and Kranias EG.** Differential phospholamban gene expression in murine cardiac compartments. Molecular and physiological analyses. *Circ Res* 77: 342–353, 1995.
20. **Lennon G, Auffray C, Polymeropoulos M, and Soares MB.** The IMAGE Consortium: an integrated molecular analysis of genomes and their expression. *Genomics* 33: 151–152, 1996.
21. **Lin Q, Schwarz J, Bucana C, and Olson EN.** Control of mouse cardiac morphogenesis and myogenesis by transcription factor MEF2C. *Science* 276: 1404–1407, 1997.
22. **Loots GG, Ovcharenko I, Pachter L, Dubchak I, and Rubin EM.** For comparative sequence-based discovery of functional transcription factor binding sites. *Genome Res* 12: 832–839, 2002.
23. **McKinsey TA, Zhang CL, and Olson EN.** Activation of the myocyte enhancer factor-2 transcription factor by calcium/calmodulin-dependent protein kinase-stimulated binding of 14-3-3 to histone deacetylase 5. *Proc Natl Acad Sci USA* 97: 14400–14405, 2000.
24. **Minajeva A, Kaasik A, Paju K, Seppet E, Lompre AM, Veksler V, and Ventura-Clapier R.** Sarcoplasmic reticulum function in determining atrioventricular contractile differences in rat heart. *Am J Physiol Heart Circ Physiol* 273: H2498–H2507, 1997.
25. **Naya FJ, Wu C, Richardson JA, Overbeek P, and Olson EN.** Transcriptional activity of MEF2 during mouse embryogenesis monitored with a MEF2-dependent transgene. *Development* 126: 2045–2052, 1999.
26. **Olgin J and Rubart M.** Remodeling of the atria and ventricles due to rate. In: *Cardiac Electrophysiology: From Cell to Bedside* (3rd ed.), edited by Zipes D and Jalife J. Philadelphia, PA: Saunders, 1999, chapt. 42 p. 364–378.
27. **Pawloski-Dahm CM, Song G, Kirkpatrick DL, Palermo J, Gulick J, Dorn GW II, Robbins J, and Walsh RA.** Effects of total replacement of atrial myosin light chain-2 with the ventricular isoform in atrial myocytes of transgenic mice. *Circulation* 97: 1508–1513, 1998.
28. **Schageman JJ, Basit M, Gallardo TD, Garner HR, and Shohet RV.** MarC-V: a spreadsheet-based tool for analysis, normalization, and visualization of single cDNA microarray experiments. *Biotechniques* 32: 338–340, 342, 344, 2002.
29. **Shelton JM, Lee MH, Richardson JA, and Patel SB.** Microsomal triglyceride transfer protein expression during mouse development. *J Lipid Res* 41: 532–537, 2000.
30. **Soonpaa MH and Field LJ.** Assessment of cardiomyocyte DNA synthesis during hypertrophy in adult mice. *Am J Physiol Heart Circ Physiol* 266: H1439–H1445, 1994.
31. **Touyz RM, Sventek P, Lariviere R, Thibault G, Farih J, Reudelhuber T, and Schiffrin EL.** Cytosolic calcium changes induced by angiotensin II in neonatal rat atrial and ventricular cardiomyocytes are mediated via angiotensin II subtype 1 receptors. *Hypertension* 27: 1090–1096, 1996.
32. **Wang Z, Yue L, White M, Pelletier G, and Nattel S.** Differential distribution of inward rectifier potassium channel transcripts in human atrium versus ventricle. *Circulation* 98: 2422–2428, 1998.
33. **Wasserman WW, Palumbo M, Thompson W, Fickett JW, and Lawrence CE.** Human-mouse genome comparisons to locate regulatory sites. *Nat Genet* 26: 225–228, 2000.